J. Fluid Mech. (2024), *vol*. 979, A49, doi:10.1017/jfm.2023.1014

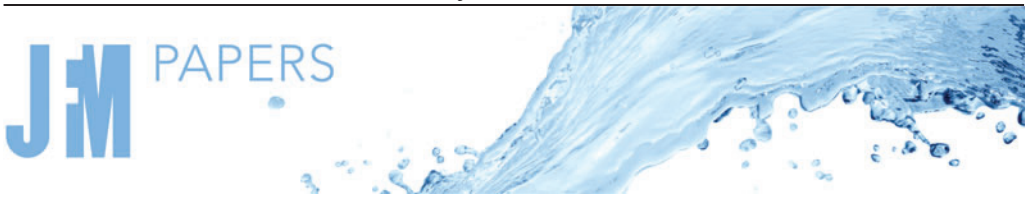

Rounded-corners-induced re-entrant non-occlusion in a horizontal tube

Dongwen Tan[1] **and Xinping Zhou**[1,2],†

[1]School of Mechanical Science and Engineering, Huazhong University of Science and Technology, Wuhan 430074, PR China

[2]State Key Laboratory of Intelligent Manufacturing Equipment and Technology, Huazhong University of Science and Technology, Wuhan 430074, PR China

(Received 8 January 2023; revised 25 October 2023; accepted 26 November 2023)

Keeping a tube from being plugged by a fluid is an important process in applications. An interesting re-entrant phenomenon for the capillary state with the occluding state sandwiching the non-occluding state from both the high- and low-Bond-number regions can appear by inserting a rod into a horizontal tube at an eccentric position (Tan *et al*., *J. Fluid Mech*, vol. 946, 2022, A7). Containers with rounded corners are very common. We theoretically investigate a situation for a horizontal open tube with rounded corner(s). The results show that a re-entrant non-occlusion at a contact angle can also appear without the insertion of any object. The competition between the rounded corner wetting/non-wetting effect and gravity effect can lead to a re-entrant non-occlusion. The re-entrant non-occlusion is affected by the shape and orientation of the rounded corner(s). For a tube with only one rounded corner, the re-entrant non-occlusion exists when the rounded corner has a not-so-large corner radius and is not in a landscape orientation. For a tube with two (or more) rounded corners, the corner(s) with the strongest corner effect will determine the existence or non-existence of the re-entrant non-occlusion. This paper provides an effective scheme for designing a high-performance capillary with corners that are not easily occluded by a fluid and removing fluid blockage from a capillary in optofluidic/microfluidic applications.

Key words: capillary flows

1. Introduction

In many processes, a tube containing multiphase fluids can be plugged by a fluid and lead to fluid blockage, thus possibly degrading the performance of the related fluid container (Zhang, Yang & Wang 2006; Mirski *et al.* 2007). The characteristic lengths of capillary

† Email address for correspondence: xpzhou08@hust.edu.cn

plugs in narrow containers can range from millimetre to micrometre sizes. Removing a fluid blockage by capillary non-occlusion is an important process. In a transverse body force field, the shape of a gas–liquid interface in a tube is more complex.

Researchers have sought effective measures to remove fluid blockages in capillaries. In theoretical research, a sharp corner, a rounded corner (a curved corner with a constant curvature radius) or a small gap can lead to liquid non-occlusion in a tube due to the effect of surface tension. Concus & Finn (1969) analysed the wetting behaviour of a sharp corner and found that for a cylindrical tube containing a sharp corner under zero gravity, a bounded occluding surface fails to exist in the tube when the condition $\alpha/2+\gamma<\pi/2$ or $\gamma-\alpha/2>\pi/2$ is satisfied, with α and γ being the corner angle and the contact angle, respectively. Concus & Finn (1987) considered two typical cross-section shapes, each of which contained a rounded corner, and found that rounded corner wetting can prevent the formation of a bounded occluding surface in the tube under zero gravity when the contact angle is smaller than the critical value. Concus & Finn (1990) discussed several examples of geometries with corners and theoretically investigated the effect of rounding a corner on the critical wetting condition. A near-rhombus-shaped cross-section with two sharp corners (Concus & Finn 1992) and a proboscis-shaped cross-section with a rounded corner (Fischer & Finn 1993) were proposed for an accurate theoretical determination of the critical contact angle for discontinuous or nearly discontinuous behaviour of liquid bulk in certain container geometries in a microgravity environment. Chen & Collicott (2004, 2006) investigated the critical wetting of a symmetrical and asymmetrical gap formed between a vane and a tank wall in a liquid propellant tank in weightlessness and determined the critical contact angle below which the wetting liquid was confined in the gap region and extended to an infinite height. In addition, they also determined the maximum gap size for a given liquid to have critical wetting. Smedley (1990) and Pour & Thiessen (2019) theoretically found that capillary non-occlusion under zero gravity can occur due to the eccentricity-induced 'wedge'-shaped slit effect, which is essentially the effect of surface tension.

Under the effect of an external force, corner wetting can still occur in a sharp or curved interior corner at a contact angle, which prevents the formation of an occluding surface in a tube. In a transverse body force field, capillary non-occlusion was theoretically observed to occur in at least one of the sharp/curved corners of a triangular (Rascón, Parry & Aarts 2016) or rectangular tube (Manning & Collicott 2015; Verma *et al.* 2020; Zhu, Zhou & Zhang 2020) that satisfies the Concus & Finn (1969) condition or an elliptical tube (Rascón *et al.* 2016) with a sufficiently large aspect ratio. Manning, Collicott & Finn (2011) proposed a flattened ice-cream-cone-shaped cylinder for liquid non-occlusion for any contact angle $\gamma\neq\pi/2$, where the sharp corner can prevent the formation of an occluding surface.

In addition to the wetting effect in a corner or a small gap, a large transverse body force is also a key factor that can cause liquid non-occlusion in a tube. Manning *et al.* (2011) was the first to theoretically determine the effect of a transverse body force on a critical non-occlusion and took a circular tube as a typical example to calculate the corresponding critical Bond number in the presence of a transverse gravity field. In addition to the case of a circular tube, in a non-circular open tube (e.g. a slit (Parry *et al.* 2012), rectangular tube (Manning & Collicott 2015; Verma *et al.* 2020; Zhu *et al.* 2020), elliptical or triangular tube (Rascón *et al.* 2016)) or in a concentric tube (Zhou *et al.* 2021), capillary non-occlusion is determined for Bond numbers larger than the critical value.

Tan *et al.* (2022) investigated the capillary non-occlusion of a horizontal tube with a rod inserted into it at an eccentric position in a downward gravity field and determined

two critical Bond numbers at a contact angle, which exhibits a phenomenon of re-entrant non-occlusion. The re-entrant non-occlusion indicates that the liquid occlusion only exists for Bond numbers between the critical ones, whereas the non-occlusion is determined for relatively low or high Bond numbers. The existence of the re-entrant non-occlusion is attributed to the insertion of a rod into a tube at an eccentric position and the integration of the two factors (i.e. eccentricity and a transverse body force) causing liquid non-occlusion. Does the re-entrant capillary non-occlusion appear in other situations without an inserted object, for example, the integrating the two factors, i.e. a transverse body force and sharp or curved corner(s)?

Because the Concus & Finn (1969) condition for the non-existence of an occluding surface in a tube with a sharp corner is not influenced by a transverse body force (see Appendix A), generally speaking, the integration of a transverse body force and only sharp corner(s) does not lead to a re-entrant non-occlusion. Containers with curved corners are very common. In reality, a corner is not ideally sharp but curved to a certain extent during the production process of a container. Moreover, a sharp corner can be deformed into a curved shape by the action of an external force (e.g. due to elastocapillarity) during use or by material ageing and can possibly be curved by the filling of limescale and the like into the corner. Accordingly, cases of curved corners are interesting and practical.

To answer the above question, we theoretically investigate the critical conditions of capillary non-occlusion for a horizontal open tube with rounded corners (representative of curved corners) and find a phenomenon of re-entrant non-occlusion following the first observation by Tan *et al.* (2022) in a horizontal tube with a rod inserted into it at an eccentric position. The critical capillary non-occluding conditions of a tube with one or two corners for different corner angles, different corner radii, different corner orientations and different contact angles are analysed. This work extends the discussion on tubes with multiple rounded corners. Notably, this research investigated a series of static equilibrium conditions under different parameters, not a process over time. The fluid dynamic responses to the change in parameters, such as Bond number, contact angle and liquid volume, in a tube can be interesting but beyond the scope of this research.

2. Mathematical model

2.1. *Geometric construction*

The cross-section of the tube studied in this research is convex. The most essential constructed geometry is a horizontal tube with only one rounded corner in a downward gravity field, as shown in figure 1(*a*). Two straight tangent edges of a circle of radius R are inclined to each other to form a corner at an angle α. The corner is blunted with an arc of a constant curvature radius $\tilde{r}$ to form a so-called rounded corner, and the corner arc is tangent to the two straight edges so that the whole boundary is smooth. The rounded corner is under the geometrical constraints $0° < \alpha < 180°$ and $0 \leq \tilde{r} \leq R$, and it degenerates to a sharp corner when $\tilde{r} = 0$. The tube cross-section with only one rounded corner is reduced to a circle of radius R when $\tilde{r} = R$. This geometry in figure 1(*a*) was theoretically studied by Concus & Finn (1987) and Smedley (1990) for its critical wetting condition under zero gravity.

A tube cross-section with two rounded corners (see figure 1*b*) is formed in the same approach as that with only one rounded corner. The tube cross-sections shown in figure 1(*a*,*b*) can be extended to cases with more than two rounded corners. For a tube with two or more rounded corners, an extra geometrical constraint should be imposed to

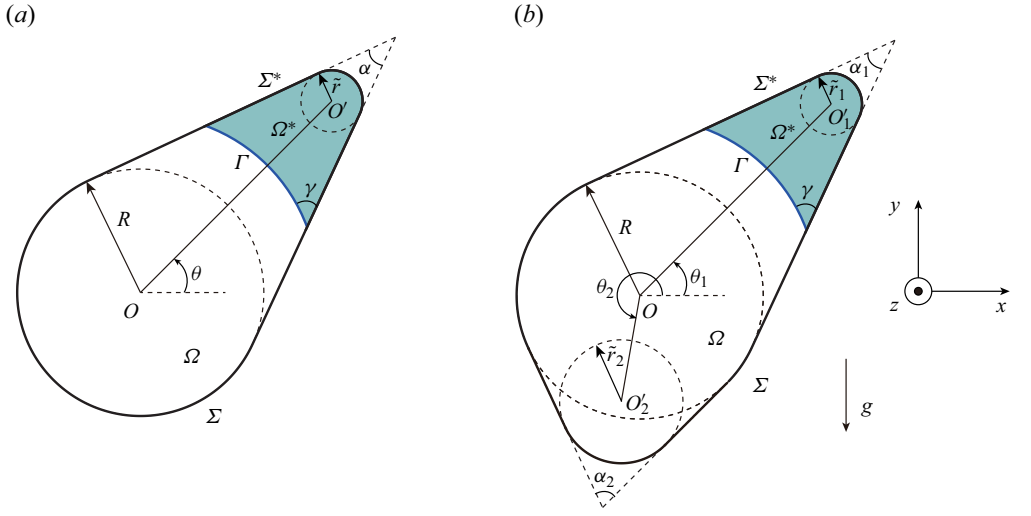

Figure 1. Schematic of a general cross-section of liquid partially filling a horizontal open tube with (*a*) a rounded corner or (*b*) two rounded corners in a downward gravity field. In (*a*), two straight tangent lines of a circle with radius R with the centre located at point O are inclined to one another to form a corner at an angle α, and the corner is rounded with a circular arc of radius $r = \tilde{r}/R$ with the centre located at point O'. Here θ is the angle between the connecting line OO' and the positive x-axis. In (*b*), two rounded corners are formed in the same approach as (*a*). We use α_1 and $r_1 = \tilde{r}_1/R$ to denote the corner angle and corner radius (corresponding to the arc centre) of one corner, respectively, and α_2 and $r_2 = \tilde{r}_2/R$ to denote the corner angle and corner radius (corresponding to the arc centre) of the other corner, respectively. Here θ_1 (θ_2) is the angle between the connecting line OO'_1 (OO'_2) and the positive x-axis. The angles θ, θ_1 and θ_2 all start from the positive x-axis and are oriented counterclockwise. The contact angle γ of the liquid on the tube wall is considered uniform. The total perimeter and area of the cross-section are Σ and Ω, respectively. The gas–liquid interface Γ meets the tube wall. The wetting perimeter and liquid area are Σ^* and Ω^*, respectively. Note that the case with a rounded corner r_1 or $r_2 = 1$ in (*b*) is equivalent to the case in (*a*), whereas the case with a rounded corner $r = 1$ in (*a*) is equivalent to a circle.

avoid overlaps between any two corners, which can be expressed as

$$\left.\begin{aligned} |\theta_i - \theta_j| + (\alpha_i + \alpha_j)/2 \le 180^\circ, \quad |\theta_i - \theta_j| < 180^\circ, \\ ||\theta_i - \theta_j| - 360^\circ| + (\alpha_i + \alpha_j)/2 \le 180^\circ, \quad |\theta_i - \theta_j| \ge 180^\circ, \end{aligned}\right\} \tag{2.1}$$

where θ is the orientation angle (see figure 1) of any rounded corner in the range $(-180^\circ, 180^\circ]$ and the subscripts i and j denote any two corners of the tube. The horizontal capillaries, each having the cross-section of an equilateral triangle studied by Rascón *et al.* (2016) and those each having the cross-section of a square studied by Manning & Collicott (2015) and Zhu *et al.* (2020), have three or four identical sharp corners, which are the specific cases of three or four corners.

2.2. *General cases*

The tube with the cross-section as constructed in the previous section is in a downward gravity field in Cartesian coordinates (x, y, z), the origin of which lies at the centre (point O, see figure 1) of the primary circular arc (radius R). The dimensionless rounding radii r, r_1 and r_2 are obtained using non-dimensionalisation by the characteristic length R as $r = \tilde{r}/R$, $r_1 = \tilde{r}_1/R$ and $r_2 = \tilde{r}_2/R$, respectively. The tube is assumed to be infinitely long and is filled with two immiscible fluids (a liquid and a gas). When the tube is occluded, the occlusions are semi-infinite plugs.

The forces of the liquid in a tube are the capillary force due to surface tension and gravity. The Bond number, which is used to characterise the relative strength of gravity to the surface tension force, is defined as

$$Bo = R^2/l_{ca}^2, \tag{2.2}$$

where the capillary length l_{ca} is given by $l_{ca} = \sqrt{\sigma/\rho g}$, where σ is the surface tension between the liquid and gas, ρ is the density difference (positive) between the liquid and gas, and g is the gravitational acceleration.

The equilibrium of the liquid droplet in this tube is attained when the total free energy E of a three-dimensional (3-D) liquid droplet in a tube given by (Finn 1986)

$$E = E_I + E_W + E_G + \lambda V, \tag{2.3}$$

reaches the minimum. E_I is the interfacial energy, E_W is the wetting energy, E_G is the gravitational potential energy, λ is the Lagrange parameter and V is the volume of the liquid. The total free energy of a liquid droplet in equilibrium in a tube is finite. When the liquid droplet plugging the tube reaches the critical condition of liquid non-occlusion, the liquid tongue can be seen to be infinitely long and have a translationally invariant cross-section. Under the critical condition, the total free energy per unit length of the tongue is equal to zero (Rascón *et al.* 2016). In other words, the 3-D problem of finding the critical condition for a tube plugging by a 3-D liquid droplet is reduced to a two-dimensional (2-D) problem of finding the condition that the minimum value of the energy functional (needed for equilibrium) of the associated 2-D droplet in the cross-section of the tube is equal to zero.

The energy functional of a 2-D droplet in the cross-section of a tube can be expressed as (Manning *et al.* 2011)

$$\Phi = |\Gamma| - |\Sigma^*|\cos\gamma + l_{ca}^{-2}\int_{\Omega^*} y\,\mathrm{d}x\,\mathrm{d}y + \lambda|\Omega^*|, \tag{2.4}$$

where y is the height of the interface. Note that the energy functional Φ is expressed in the form of lengths in (2.4). The full form of the energy of a 2-D droplet should be $\sigma\Phi$, and (2.4) can be obtained by dividing all terms of the energy equation by the surface tension σ. The Lagrange parameter λ in (2.4) is written as

$$\lambda = \frac{1}{|\Omega|}\left(|\Sigma|\cos\gamma - l_{ca}^{-2}\int_{\Omega} y\,\mathrm{d}x\,\mathrm{d}y\right). \tag{2.5}$$

Minimisation of the energy functional Φ can lead to the Young–Laplace equation (Finn 1986; Bhatnagar & Finn 2016) describing the shape of the gas–liquid interface in two dimensions in the form given by

$$\left(\frac{y_x}{(1+y_x^2)^{0.5}}\right)_x = l_{ca}^{-2}y + \lambda. \tag{2.6}$$

For a given contact angle, at a Bond number, in the cross-section of a tube, there is possibly more than one interface (described using (2.6)) with the contact angle condition

$$\boldsymbol{\nu}\cdot\frac{\nabla y}{(1+|\nabla y|^2)^{0.5}} = \cos\gamma, \tag{2.7}$$

satisfied, where $\boldsymbol{\nu}$ is the unit exterior normal to the tube on the perimeter Σ of the cross-section. The values of the energy functional are calculated using (2.4) for all

possible interfaces. The minimum Φ_{min} of the values of the energy functional is determined, and the corresponding interface (Γ) and other parameters (Ω^* and Σ^*) are chosen. The tube is non-occluding when $\Phi_{min} < 0$, while a liquid plug is permitted when $\Phi_{min} > 0$ (Manning *et al.* 2011). If the Bond number satisfies the relationship

$$\Phi_{min} = 0, \tag{2.8}$$

then it is just the critical Bond number for non-occluding. The key process of the computational procedure for determining the critical Bond number(s) of a tube is to plot the variational curve of Φ_{min} as a function of Bond number ranging from zero to a large enough value and to determine the point(s) satisfying (2.8) if the point(s) exist (Tan *et al.* 2022).

For a tube with rounded corners, different solutions to (2.8) could be obtained, which correspond to different types of capillary non-occlusion for various Bond numbers. If $\Phi_{min} < 0$ for all Bond numbers (that is, there is not one solution of (2.8) as shown in figure 2*c*) at a contact angle, then capillary plugging does not exist in a tube, which corresponds to the unconditional liquid non-occlusion at the contact angle regardless of the Bond number. $\Phi_{min} > 0$ at a Bond number permits at least a critical Bond number (satisfying (2.8)) between the Bond number and a large enough Bond number that has to cause liquid non-occlusion, implying $\Phi_{min} < 0$. If there is only one solution of (2.8) obtained for a contact angle, corresponding to one critical Bond number Bo_c, capillary plugging does not exist when the following condition is satisfied (Manning *et al.* 2011; Manning & Collicott 2015; Rascón *et al.* 2016; Zhu *et al.* 2020; Zhou *et al.* 2021):

$$Bo > Bo_c. \tag{2.9}$$

In other words, the tube is non-occluding in a single region of sufficiently high Bond numbers (Bo_c, $+\infty$) (see figure 2*a*). If there are two solutions of (2.8) obtained for a contact angle, corresponding to the lower and upper critical Bond numbers (Bo_{cl} and Bo_{cu}, $Bo_{cl} < Bo_{cu}$), then capillary plugging does not exist when the following condition is satisfied (Tan *et al.* 2022):

$$Bo > Bo_{cu} \quad \text{or} \quad Bo < Bo_{cl}. \tag{2.10}$$

The case admitting two critical Bond numbers exhibits a re-entrant non-occlusion with different Bond numbers. That is, in addition to the region of higher Bond numbers (Bo_{cu}, $+\infty$), the tube is also determined to be non-occluding in a second region of lower Bond number $[0, Bo_{cl})$ (see figure 2*b*).

In summary, for a tube at a contact angle, no critical Bond number corresponds to the non-occlusion regardless of Bond numbers, i.e. unconditional non-occlusion, one critical Bond number corresponds to the non-occlusion for a single Bond number region, and two critical Bond numbers correspond to the non-occlusion for two distinct regions, i.e. the re-entrant non-occlusion.

2.3. *Zero-gravity cases*

2.3.1. *Rounded corner wetting/non-wetting under zero gravity*

We consider the condition of zero gravity (i.e. $Bo = 0$) for the prediction of the type of capillary non-occlusion. As shown in figure 2, the unconditional non-occlusion and re-entrant non-occlusion require the tube to be non-occluding at a zero Bond number (i.e. $\Phi_{min}(Bo = 0) < 0$), while for the type of non-occlusion for a single region, the liquid plug is permitted at a zero Bond number (i.e. $\Phi_{min}(Bo = 0) > 0$). Furthermore, we have proven

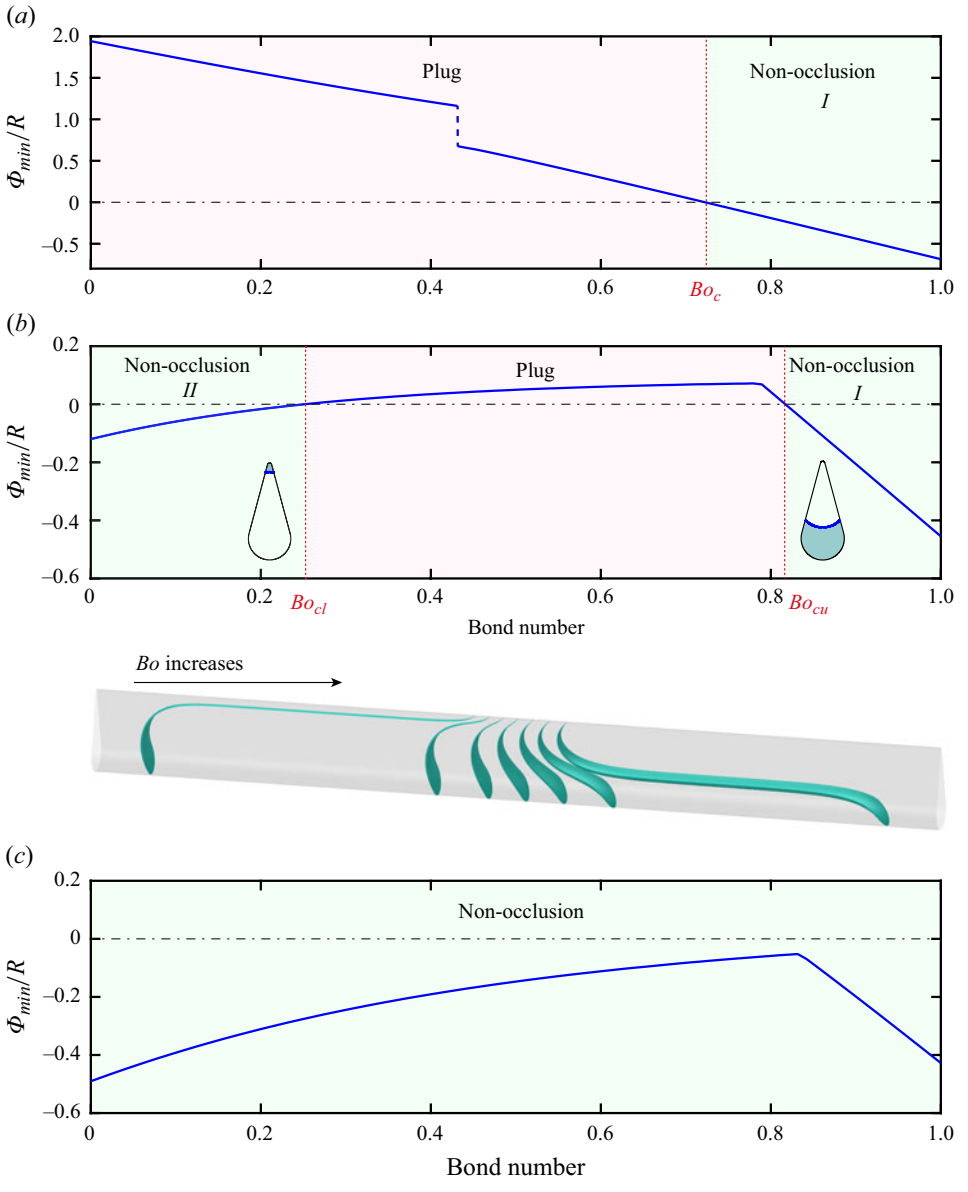

Figure 2. Three types of capillary non-occlusion for Bond numbers: (*a*) non-occlusion for a single region, (*b*) non-occlusion for two distinct regions (re-entrant non-occlusion) and (*c*) unconditional liquid non-occlusion. For the horizontal tube with only one rounded corner ($\alpha = 30°$, $r = 0.1$ and $\theta = 90°$), the contact angle is given by (*a*) $\gamma = 75°$, (*b*) $\gamma = 55°$ and (*c*) $\gamma = 35°$. The red dotted lines denote the solutions of (2.8) (i.e. $Bo = Bo_c$ in (*a*) and $Bo = Bo_{cl}$ and $Bo = Bo_{cu}$ in (*b*)). In (*b*), the non-occluded liquid configurations on the left and right correspond to $Bo = Bo_{cl}$ and $Bo = Bo_{cu}$, respectively. The 3-D interfaces of the liquid plug as the Bond number gradually increases are computed using Surface Evolver (Brakke 1992) and integrated in a horizontal tube.

(see Appendix B) that under zero gravity, for a tube constructed as described in § 2.1, only the 'corner liquid configuration' such as shown in figure 3 can reach the minimum energy of the 2-D droplet $\Phi_{min}(Bo = 0)$. This means that the capillary non-occlusion under zero gravity depends on whether the energy of the 'corner liquid configuration' is negative. If so, the corner wetting/non-wetting will be permitted in the corresponding corner, where

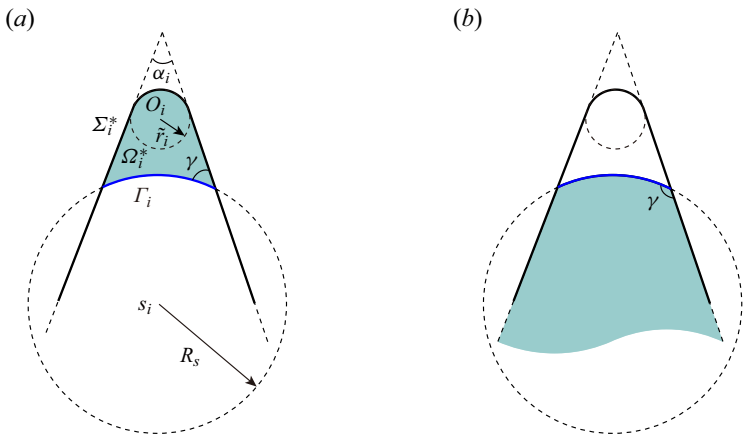

Figure 3. Schematic of the 'corner liquid configuration' in the ith rounded corner of a tube under zero gravity for (*a*) the wetting case ($\gamma < 90°$) and (*b*) the non-wetting case ($\gamma > 90°$). For the 'corner liquid configuration', the contact points are prescribed on the two straight edges of a corner. The contact angles in (*a*) and (*b*) are complementary angles.

the fluid (i.e. the liquid for the wetting case or the gas for the non-wetting case) is confined to the corner and extends to an infinite length, leading to the capillary non-occlusion. It follows that the corner wetting/non-wetting under zero gravity must be permitted in the tube when the re-entrant or unconditional non-occlusion occurs at a contact angle.

Since the interface (described using (2.6)) of the 2-D droplet is a circular arc under zero gravity (Concus & Finn 1990), the energy of the 'corner liquid configuration' can be theoretically given.

Note that the case of two or more corners should be under the geometrical constraint (2.1). For a tube with n ($n \geq 1$) rounded corners under zero gravity, the expression of the Lagrange parameter (2.5) is reduced to $\lambda = |\Sigma| \cos\gamma / |\Omega|$, which is rewritten as

$$\lambda = \frac{2\cos\gamma}{R} \frac{2\pi + \sum_{i=1}^{n} [\alpha_i - \pi + 2(1 - r_i)\cot(\alpha_i/2) + r_i(\pi - \alpha_i)]}{2\pi + \sum_{i=1}^{n} [\alpha_i - \pi + 2(1 - r_i^2)\cot(\alpha_i/2) + r_i^2(\pi - \alpha_i)]}. \tag{2.11}$$

and the interface is a circular arc, the radius of which can be written as

$$R_s = \frac{1}{\lambda} = R \frac{2\pi + \sum_{i=1}^{n} [\alpha_i - \pi + 2(1 - r_i^2)\cot(\alpha_i/2) + r_i^2(\pi - \alpha_i)]}{2\cos\gamma \left\{ 2\pi + \sum_{i=1}^{n} [\alpha_i - \pi + 2(1 - r_i)\cot(\alpha_i/2) + r_i(\pi - \alpha_i)] \right\}}. \tag{2.12}$$

For the wetting case, according to the calculation, the 'corner liquid configuration' exists in the ith corner when satisfying the condition

$$\gamma < \cos^{-1}\left(\frac{Rr_i + \sqrt{2R_s^2 - (Rr_i)^2}}{2R_s} \right). \tag{2.13}$$

The upper limit of the contact angle in (2.13) is determined when the endpoints of the interface are just on the intersections between the corner arc and the corner straight edges.

As the energies of the liquid configurations identified by two complementary contact angles (such as figure 3*a*,*b*) are equal (Manning *et al* 2011; Tan *et al*. 2022), it suffices to consider only the wetting case when calculating the energy for the 'corner liquid configuration'.

Denote ϕ as the energy functional for the 'corner liquid configuration'. For the wetting case, if the 'corner liquid configuration' exists in the ith rounded corner (i.e. (2.13) is satisfied), the corresponding energy functional ϕ_i is expressed as

$$\phi_i = |\Gamma_i| - |\Sigma_i^*| \cos\gamma + \lambda |\Omega_i^*|, \tag{2.14}$$

where Γ_i, Σ_i^* and Ω_i^* are the interface, the wetting perimeter and the liquid area in the ith rounded corner, respectively. Based on the geometric relationship shown in figure 3(*a*), the parameters can be obtained as

$$|\Gamma_i| = R_s(\pi - \alpha_i - 2\gamma), \tag{2.15a}$$

$$|\Sigma_i^*| = \frac{2R_s\cos\gamma - 2r_i}{\tan(\alpha_i/2)} - 2R_s\sin\gamma + r_i(\pi - \alpha_i), \tag{2.15b}$$

$$|\Omega_i^*| = \frac{R_s^2\cos\gamma\cos(\gamma + \alpha_i/2)}{\sin(\alpha_i/2)} - \frac{1}{2}R_s^2(\pi - \alpha_i - 2\gamma) - \frac{r_i^2}{\tan(\alpha_i/2)} + \frac{1}{2}r_i^2(\pi - \alpha_i). \tag{2.15c}$$

By substituting (2.15) into (2.14), we can calculate the energy functional ϕ_i.

The corner wetting/non-wetting under zero gravity is permitted in the ith corner when $\phi_i < 0$. We consider the critical case

$$\phi_i = 0. \tag{2.16}$$

For wetting liquids ($\gamma < 90°$), the critical contact angle $\gamma_{i,cr}$ of a rounded corner can be obtained by solving (2.16) with the given geometric parameters of the tube. Then, the corner wetting in the ith corner is permitted for $\gamma < \gamma_{i,cr}$, while it is not permitted for $\gamma_{i,cr} < \gamma < 90°$ (Finn 1986; Concus & Finn 1990). Regarding non-wetting liquids ($\gamma > 90°$), the critical contact angle $\gamma_{i,cr}^*$ can be obtained by the relation $\gamma_{i,cr}^* = 180° - \gamma_{i,cr}$ (Tan *et al*. 2022). Likewise, the corner non-wetting in the ith corner is permitted for $\gamma > \gamma_{i,cr}^*$ but is not permitted for $90° < \gamma < \gamma_{i,cr}^*$. If no such critical contact angle $\gamma_{i,cr}$ or $\gamma_{i,cr}^*$ exists between 0° and 180°, the corner wetting/non-wetting under zero gravity will not occur in the ith corner for any liquid.

Note that for the special case of the corner with $r = 0$ (the corner being a sharp corner), there is no need to solve (2.16) for the critical contact angle, as the corner wetting/non-wetting is permitted in a sharp corner only if satisfying the Concus & Finn (1969) condition, i.e. $\gamma < \pi/2 - \alpha/2$ or $\gamma > \pi/2 + \alpha/2$. From (2.12), (2.14), (2.15) and (2.16), it can be seen that for a rounded corner, the critical contact angle is affected by the other corners in the tube, whereas for a sharp corner, it only depends on the sharp corner angle according to the Concus & Finn (1969) condition.

If some corners in a tube have the same critical contact angle, these corners are considered to have an equal corner effect, as they identify the same contact angle ranges in which the corner wetting/non-wetting under zero gravity is permitted. For a pair of corners, the geometric condition for them to have the equal corner effect is given by

$$\phi_i = \phi_j = 0. \tag{2.17}$$

Setting the radii $r_{i,e}$ and $r_{j,e}$ of the two corners as variables and fixing the other geometric parameters of the tube, a relation between the two radii $r_{i,e}$ and $r_{j,e}$ can be obtained based

on (2.17). Then, these two corners have an equal corner effect (e.g. the points on the black solid line in figure 10*a*). For the tube with only two corners, the two corners having an equal corner effect may lead to the disappearance of the re-entrant non-occlusion, which is discussed in detail in § 3.2.1. For a rounded corner in a tube with other parameters fixed, a smaller corner radius (or a smaller corner angle) for the corner leads to a larger contact angle range for the corner wetting/non-wetting under zero gravity, which corresponds to a stronger corner effect. We note that the terms 'equal' or 'stronger' used here only indicate the same or the larger contact angle range for corner wetting/non-wetting but do not refer to the performance of the corner flow in dynamics.

2.3.2. *Critical contact angle and limiting geometric condition for a tube*

For the tube with n corners, the energy of the 'corner liquid configuration' for each corner would be calculated, and then the minimum energy is obtained as $\Phi_{min}(Bo = 0) = \min(\phi_1, \phi_2, \ldots, \phi_i, \ldots, \phi_n)$. Note that for some corners in a tube, the 'corner liquid configuration' may not exist (i.e. it may not satisfy (2.13)) and, thus, the calculations for the corresponding corners should be abandoned.

The condition for the capillary non-occlusion under zero gravity can be expressed as

$$\Phi_{min}(Bo = 0) = \min(\phi_1, \phi_2, \ldots, \phi_i, \ldots, \phi_n) < 0, \tag{2.18}$$

which implies that if (one of the n corners of) the tube permits the corner wetting/non-wetting under zero gravity, the non-occlusion will occur for the tube. In addition, condition (2.18) is necessary for the occurrence of the re-entrant or unconditional non-occlusion at a contact angle. With the given geometric parameters, the critical contact angle for the corner wetting/non-wetting in a tube is obtained by solving

$$\Phi_{min}(Bo = 0) = \min(\phi_1, \phi_2, \ldots, \phi_i, \ldots, \phi_n) = 0. \tag{2.19}$$

For wetting liquids ($\gamma < 90°$), the solution of (2.19) obtained as γ_{cr} is the maximum value of $\gamma_{i,cr}$ (where $i = 1, 2, \ldots, n$). Likewise, for non-wetting liquids ($\gamma > 90°$), the critical contact angle γ^*_{cr} is the minimum value of $\gamma^*_{i,cr}$ (where $i = 1, 2, \ldots, n$) and follows the relation $\gamma^*_{cr} = 180° - \gamma_{cr}$. Then, the corner wetting/non-wetting under zero gravity could occur for contact angles in the range $\gamma < \gamma_{cr}$ and $\gamma > \gamma^*_{cr}$, whereas it will not occur for $\gamma_{cr} < \gamma < \gamma^*_{cr}$. If γ_{cr} or γ^*_{cr} does not exist between 0° and 180°, the corner wetting/non-wetting under zero gravity will not occur in the tube for any contact angle, which also implies that the tube will not permit the re-entrant non-occlusion and unconditional non-occlusion. Then, a limiting geometric condition for the corner wetting/non-wetting under zero gravity in the tube can be determined by letting $\gamma_{cr} = 0°$, i.e. solving the equation

$$\Phi_{min}(Bo = 0,\ \gamma = 0°) = 0. \tag{2.20}$$

It suffices to solve (2.20) to obtain the limiting geometric condition, as the equation for the complementary case $\Phi_{min}(Bo = 0,\ \gamma = 180°) = 0$ is equivalent to (2.20).

3. Results and discussion

In this section, we investigate the effects of different parameters (including wettability and geometric parameters) on non-occlusions, especially the case of two non-occluding regions for Bond numbers, i.e. the re-entrant non-occlusion (see figure 2*b*). The tubes with only one corner and two corners are analysed in §§ 3.1 and 3.2, respectively. In addition, § 3.3 provides a qualitative discussion on the tube with multiple (more than two) corners.

3.1. *A rounded corner*

We begin by considering a tube with only one rounded corner. We comprehensively analyse the effect of the geometric parameters of the corner (i.e. the corner angle, the corner radius and the corner orientation) on the capillary non-occlusion and then present the phase diagrams of the types of capillary non-occlusion in a parameter space (γ, r).

3.1.1. *Effect of the corner shape*

Consider a horizontal open tube with only one rounded corner. The corner shape is identified by the corner angle and the constant corner radius. Figure 4 shows the critical Bond numbers of the open tubes for different corner radii and corner angles with a portrait corner orientation ($\theta = 90°$). Interestingly, followed by the first observation in a horizontal eccentric tube (Tan *et al.* 2022), the re-entrant non-occlusion is also observed for the tube with a rounded corner (for example, the cases of $0 < r \leq 0.5$ in figure 4*a–c*).

The plot of a critical Bond number line exhibits different types of capillary non-occlusion for Bond numbers at different contact angles. Take the case of $\alpha = 30°$ and $r = 0.1$ as an example (see the thick red line in figure 4*a*). The critical Bond number line intersects the γ axis at two points, and the values of γ of the two intersection points are γ_{cr} ($<90°$) and γ_{cr}^{*} ($>90°$), which can be theoretically determined by solving (2.19) and satisfy $\gamma_{cr} = 180° - \gamma_{cr}^{*}$, as mentioned in § 2.3.2. For the contact angle in the range $\gamma_{cr} < \gamma < \gamma_{cr}^{*}$, only one critical Bond number is identified, which corresponds to the non-occlusion for a single Bond number region. The lower limit of the contact angle identifying two critical Bond numbers is denoted by γ_l (e.g. the contact angle value of point L on the thick red line in figure 4*a*). For $\gamma_l < \gamma < \gamma_{cr}$, two critical Bond numbers are identified, which correspond to the re-entrant non-occlusion. For $\gamma > \gamma_{cr}^{*}$ or $\gamma < \gamma_l$, no critical Bond number is identified, which corresponds to the unconditional non-occlusion. The results indicate that the re-entrant non-occlusion and the unconditional non-occlusion only occur for contact angles $\gamma < \gamma_{cr}$ or $\gamma > \gamma_{cr}^{*}$, i.e. the contact angles permitting the corner wetting in the tube under zero gravity.

The re-entrant non-occlusion arises from the competition between the rounded corner wetting/non-wetting effect and the gravity effect. Consider the wetting case. For the tube with a top corner, the corner wetting effect tends to pull the wetting liquid in the top corner, whereas gravity tends to pull the liquid down to the bottom, which leads to competition between the corner wetting effect and gravity effect to place the liquid. For $\gamma_l < \gamma < \gamma_{cr}$, gravity vanishes at a zero Bond number, and the corner wetting leads to the non-occlusion of the tube. When the Bond number ranges from zero to a small value less than Bo_{cl} (the lower critical Bond number), the corner wetting effect dominates over the gravity effect and still keeps the liquid in the top rounded corner (see, e.g., the non-occluded liquid configuration of point A in figure 4*a*), which prevents the formation of an occluding surface. When the Bond number is betwee Bo_{cl} and Bo_{cu} (the lower and upper critical Bond numbers), the liquid under the offsetting effects of corner wetting and gravity can occlude the tube. Regarding liquid plugging, the upper and lower tongues of the plugged capillary surface directly computed via Surface Evolver (Brakke 1992) at $\gamma = 55°$ gradually become shorter and longer, respectively, for a larger Bond number (see figure 4*a*). When Bo approaches the lower (upper) critical Bond number, the upper (lower) tongue is much longer than the lower (upper) tongue (see also figure 2*b*). For Bond numbers larger than Bo_{cu}, the gravity effect dominates over the rounded corner wetting effect, and the liquid is pulled down and spreads along the bottom of the tube (see, e.g., the non-occluded liquid configuration of point B in figure 4*a*), which leads to liquid non-occlusion. Naturally, the re-entrant non-occlusion is observed with the Bond number

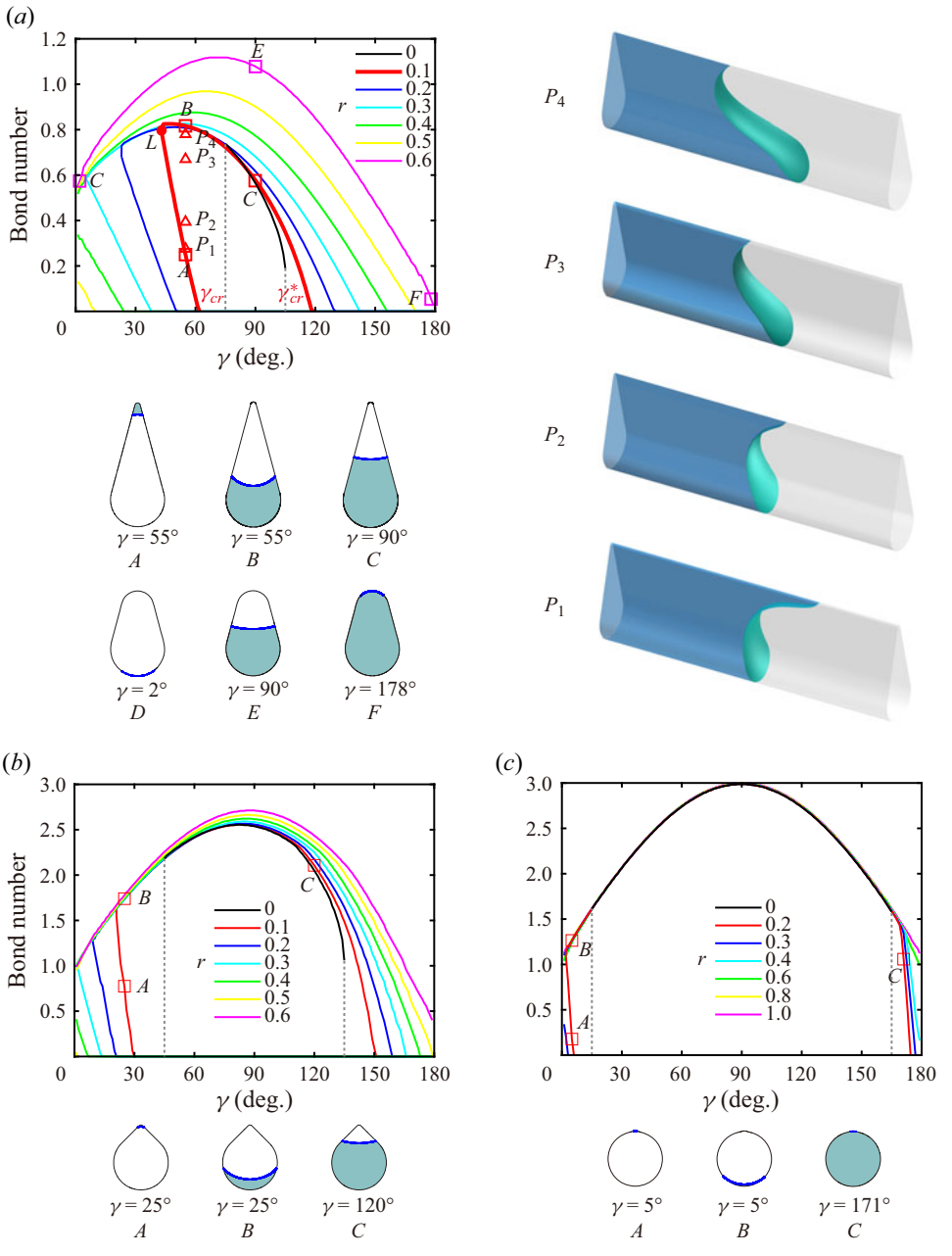

Figure 4. Critical Bond numbers of a horizontal tube with only one rounded interior corner for different corner radii and different corner angles: (*a*) $\alpha = 30°$, (*b*) $\alpha = 90°$ and (*c*) $\alpha = 150°$ at $\theta = 90°$ versus contact angle. The grey dotted lines are the critical contact angles of the Concus & Finn (1969) condition, i.e. (*a*) $\gamma = 75°$ and $\gamma = 105°$, (*b*) $\gamma = 45°$ and $\gamma = 135°$ and (*c*) $\gamma = 15°$ and $\gamma = 165°$. In (*a*), for the case of $r = 0.1$ at $\gamma = 55°$, points P_1, P_2, P_3 and P_4 correspond to the capillary states permitting the liquid plug, the 3-D interfaces (an oblique view) of which are directly computed via Surface Evolver (Brakke 1992), as shown on the right-hand side.

varying from zero to a sufficiently large value, which is validated by direct computation via Surface Evolver (Brakke 1992). Details about the Surface Evolver calculation can be seen in the supplementary material available at https://doi.org/10.1017/jfm.2023.1014.

As shown in figure 4, when the re-entrant non-occlusion occurs (for $\gamma_l < \gamma < \gamma_{cr}$), the lower critical Bond number increases as the contact angle decreases because the condition of being more hydrophilic is more favourable for corner wetting, and a greater gravity is needed to pull the wetting liquid down to occlude the tube. For the non-wetting liquid with $\gamma > \gamma_{cr}^*$, the competition between the corner non-wetting effect and gravity effect does not exist because both effects tend to pull the non-wetting liquid out of the top rounded corner, which prevents the formation of an occluding surface and leads to the unconditional liquid non-occlusion regardless of the Bond number.

For the tube with only one corner, the re-entrant non-occlusion can exist for the not-so-large corner radius r but does not exist when r reduces to zero (sharp corner). As shown in figure 4(*a–c*), all the cases with $r = 0$ permit the unconditional non-occlusion but do not exhibit the re-entrant non-occlusion. In addition, the critical Bond number only exists within the range $\pi/2 + \alpha/2 < \gamma < \pi/2 - \alpha/2$. This implies that the computed results of the contact angle range for the unconditional non-occlusion are consistent with the Concus & Finn (1969) condition (i.e. $\gamma < \pi/2 - \alpha/2$ or $\gamma > \pi/2 + \alpha/2$). This range also matches with the 'non-occluding pipe' condition (Manning *et al*. 2011). The 'non-occluding pipe', of which the shape is the same as with the sharp-corner cases in figure 4 but the sharp corner is in an opposite orientation, was theoretically proposed by Manning *et al*. (2011) to keep non-occluding under gravity through the sharp corner wetting effect. In fact, when the contact angle satisfies the Concus & Finn (1969) condition of the sharp corner of a tube, the capillary non-occlusion will occur regardless of corner orientation and gravity (proven in Appendix A), which leads to an unconditional non-occlusion and prevents the re-entrant non-occlusion.

For the tube permitting the corner wetting/non-wetting, a larger corner radius or a larger corner angle reduces the effectiveness of corner wetting/non-wetting, which leads to liquid occlusion over a broader range of contact angles and Bond numbers (see figure 4). Too large a corner radius will not lead to corner wetting/non-wetting at a zero Bond number for any contact angle, thereby preventing the appearance of re-entrant non-occlusion. For the case of only one rounded corner, the limiting corner radius for corner wetting/non-wetting under zero gravity can be obtained by solving (2.20). As shown in figure 5, for any corner with $0° < \alpha < 180°$, the corner wetting/non-wetting under zero gravity can occur in the tube provided that the corner radius satisfies $r \leq 0.5$. Moreover, under the condition of the corner not in a landscape orientation (i.e. $\theta \neq 0°$ and 180°), the limiting corner radius for corner wetting/non-wetting (see the blue curve in figure 5) also indicates the maximum corner radius for existence of the re-entrant non-occlusion in the tube. The effect of the corner orientation is discussed in the following section.

3.1.2. *Effect of the corner orientation*

To study the effect of the orientation of the rounded corner, figure 6 shows the critical Bond number lines of an open tube with a rounded corner at an orientation angle θ ranging from $-90°$ through 0° to 90°. The critical Bond number for a contact angle γ at an orientation θ is equal to that for the complementary contact angle $180° - \gamma$ at the opposite orientation $-\theta$ (e.g. the critical points A and D have the same value of Bond number, and the critical points B and C have the same value of Bond number). According to Tan *et al*. (2022), a gas–liquid interface for an orientation angle $-\theta$ and a contact angle $180° - \gamma$ that is

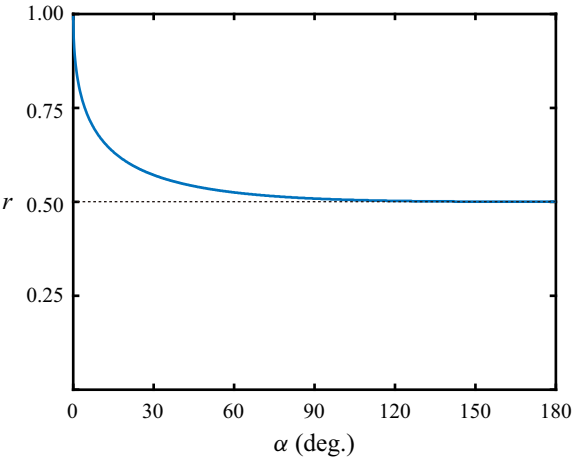

Figure 5. The limiting corner radii for permitting the corner wetting/non-wetting under zero gravity with corner angles varying in the range $0° < \alpha < 180°$. The blue curve theoretically determined by (2.20) denotes the limiting corner radii for various corner angles. The black dotted line denotes the straight line $r = 0.5$. The limiting corner radius decreases monotonically as the corner angle increases, and the limiting corner radius approaches 0.5 when the corner angle approaches 180°.

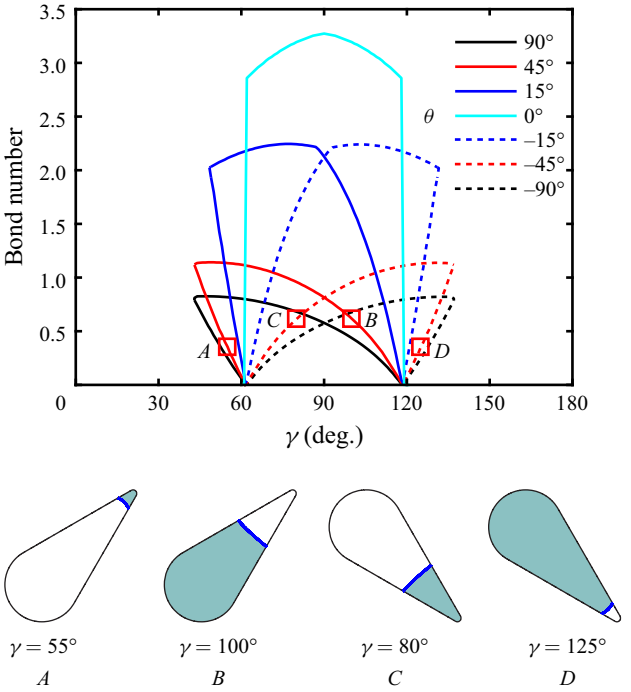

Figure 6. Critical Bond numbers of a horizontal tube with only one rounded interior corner with angle $\alpha = 30°$ and corner radius $r = 0.1$ for different orientation angles θ ranging from $-90°$ through 0° to 90° versus contact angle.

symmetric to a given interface for an orientation angle θ and a contact angle γ can be found (see, e.g., the non-occluded liquid configurations of A and D, or the non-occluded liquid configurations of B and C), and the values of the energy functional calculated from (2.4) for the two sets of orientation angles and contact angles are equal. Therefore, the

critical Bond numbers satisfying (2.8) for the two sets of orientation angles and contact angles are equal, which can also be seen in figure 6. An orientation angle range from 0° to 90° is sufficient for research on the effect of the orientation angle of the corner for the case of only one corner.

In figure 6, the intersection points of the critical Bond number line and the γ axis are fixed with θ varying, because the critical contact angles for corner wetting/non-wetting under zero gravity (i.e. γ_{cr} and γ_{cr}^{*}) are independent of θ. With θ decreasing from 90° to 0°, two characteristics of the change in the critical Bond number lines are worth considering. First, the contact angle range of the re-entrant non-occlusion tends to be narrower, and the re-entrant non-occlusion does not occur for the corner in a landscape orientation ($\theta = 0°$ or 180°). Since the re-entrant non-occlusion arises from the competition between the corner wetting effect and gravity effect, the gravity effect to pull the liquid out of the corner against the corner wetting effect is weakened with θ varying from 90° to 0°, thus causing a reduction in the permitting contact range for the re-entrant non-occlusion. This characteristic means that the corner approaching the landscape orientation is beneficial to liquid non-occluding at a moderate Bond number. Second, the upper critical Bond number Bo_{cu}, especially for contact angles $\gamma_{cr} < \gamma < \gamma_{cr}^{*}$ (for which only one critical Bond number is identified), becomes larger. This means that the variation in θ from 90° to 0° is not favourable for removing a liquid plug, especially for contact angles close to 90°. Similar characteristics appear in the tubes with other geometries. For example, for a rectangular (Manning & Collicott 2015) or an elliptical (Rascón *et al*. 2016) occluded tube, removing a liquid plug requires a lower gravity for the tube in a portrait orientation (long side of the rectangle or major axis of the ellipse parallel to the direction of gravity) than that in a landscape orientation (long side of the rectangle or major axis of the ellipse perpendicular to the direction of gravity).

For $\theta = 0°$, the critical Bond number line is symmetric with respect to the line $\gamma = 90°$, which is attributed to the geometric symmetry of the tube with respect to the vertical axis. For two supplementary contact angles, the corresponding two critical Bond numbers are equal (both satisfy (2.8)) due to this symmetry.

From the above results, we conclude that for the tube with only one rounded corner, the re-entrant non-occlusion will occur, if the rounded corner wetting/non-wetting condition is satisfied and the rounded corner is not in a landscape orientation.

3.1.3. *Phase diagram*

As mentioned previously, the capillary non-occlusion prescribed in this paper can be classified into three types according to the number of the critical Bond number Bo_c, i.e. unconditional liquid non-occlusion (corresponding to zero Bo_c), non-occlusion for a single Bond number region (corresponding to one Bo_c) and non-occlusion for two Bond number regions (or, say, re-entrant non-occlusion corresponding to two Bo_c). To demonstrate the effect of the corner shape, corner orientation and wettability on the types of the capillary non-occlusion more clearly, figure 7 illustrates the number of Bo_c in a parameter space (γ, r).

As shown in figure 7(*a*), the zero-Bo_c cases and the two-Bo_c cases would not exist for a large corner radius ($r > 0.57$), regardless of the magnitude of the contact angle. The boundary line (black solid line) of the one-Bo_c region does not change with θ (just as γ_{cr} and γ_{cr}^{*} do not change with θ as shown in figure 6), while the two-Bo_c region in the parameter space decreases with θ decreasing from 90° until it disappears when $\theta = 0°$. The two-Bo_c cases only occur at $\gamma < 90°$ for $0° < \theta \leq 90°$, and the range of r corresponding to the case becomes larger with decreasing γ. The two-Bo_c cases will occur at $\gamma > 90°$ for

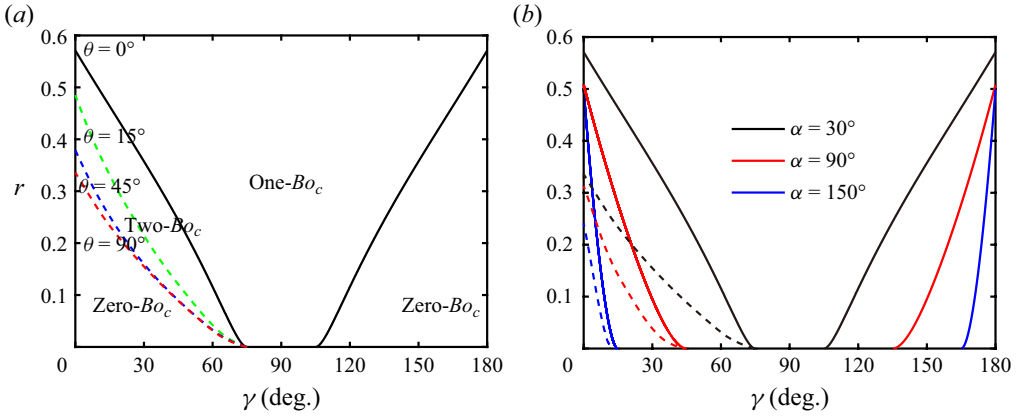

Figure 7. Phase diagram of the cases having different numbers of Bo_c in a parameter space (γ, r) for (a) different orientation angles $0^\circ \leq \theta \leq 90^\circ$ at $\alpha = 30^\circ$ and for (b) the orientation angle $\theta = 90^\circ$ at different corner angles $\alpha = 30^\circ$, 90° and 150°. In (a), boundaries between different regions are presented, and the different line colours correspond to the cases for different θ. The dashed line is the boundary between the left zero-Bo_c region and the two-Bo_c region. The solid line, which does not change with different θ, is the boundary between the two-Bo_c region and the one-Bo_c region and is also the boundary between the one-Bo_c region and the right zero-Bo_c region. Note that the dashed line for $\theta = 0^\circ$ coincides with the left part of the solid line. In (b), the meanings of the different line types are the same as those in (a), and the different line colours correspond to the cases for different α.

$-90^\circ \leq \theta < 0^\circ$, and the region is symmetric to that for $0^\circ < \theta \leq 90^\circ$ with respect to the vertical line $\gamma = 90^\circ$.

As shown in figure 7(b), $\theta = 90^\circ$ is used as an example to analyse the effect of the corner angle on the boundary lines. With an increasing corner angle, both the two-Bo_c region (between the solid and dashed curves of the same colour) and the zero-Bo_c region (below the dashed curve) are reduced. It can be concluded that a smaller corner angle can lead to an effective increase in the possibility of unconditional liquid non-occlusion in a tube with only one corner.

3.2. *Two rounded corners*

In this section, we consider a tube with only two rounded corners. Each corner is determined by three geometric parameters (the corner angle, the corner radius and the orientation angle of the corner), and thus the geometry of the tube with two corners relates to a six-dimensional parameter space, which corresponds to numerous cases. However, we focus on the re-entrant non-occlusion only for some typical cases. In the following, we first keep the two corners at the same angle. Then, we analyse the cases with the two corners having different angles and different rounding radii. Phase diagrams are then given to illustrate the existence of the re-entrant non-occlusion for tubes with different geometric parameters.

3.2.1. *Two rounded corners with the same corner angle*

For a vertically symmetrical tube with two equal corner angles, the critical Bond numbers for various corner radii are shown in figure 8(a). It is found that the re-entrant non-occlusion does not occur for any contact angle when $r_1 = r_2$.

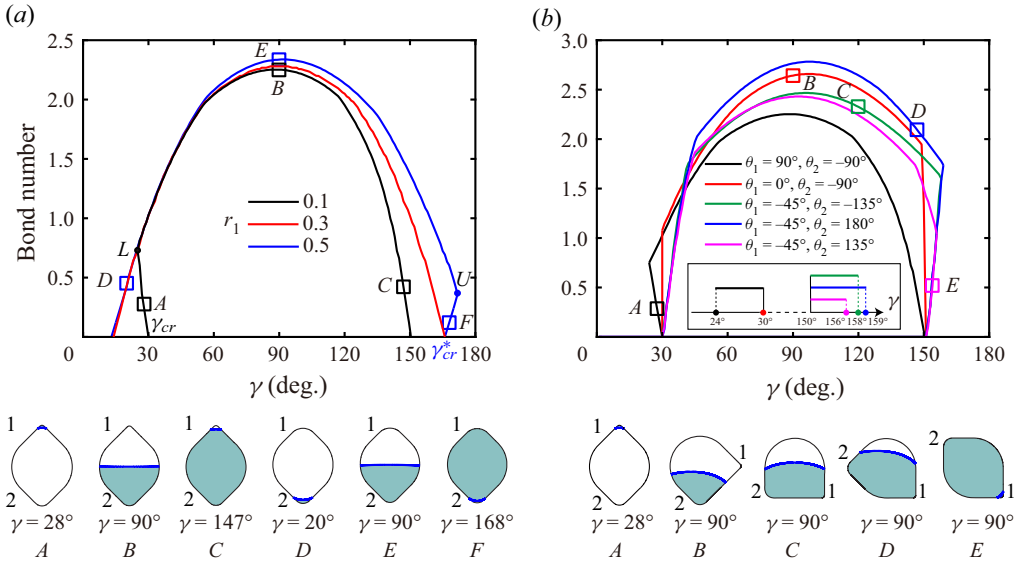

Figure 8. Critical Bond numbers of a horizontal tube with only two rounded corners with the same angle ($\alpha_1 = \alpha_2 = 90°$) versus contact angle for (*a*) $r_2 = 0.3$ and different values of r_1 at $\theta_1 = 90°$ and $\theta_2 = -90°$ and (*b*) different combinations of the orientation angles θ_1 ranging between 0° and 90° and θ_2 ranging between −180° and −90°. In the inset of (*b*), the contact angle ranges of the re-entrant non-occlusion for all the curves are given.

According to the previous sections, the rounded corner wetting/non-wetting effect and gravity effect compete to place the liquid, which can lead to the re-entrant non-occlusion. Consider a tube with only two corners, of which one is in an upper orientation ($0 < \theta_1 < 180°$) and the other is in a lower orientation ($-180° < \theta_2 < 0°$), as the cases shown in figure 8(*a*). If both the upper and lower corners permit the corner wetting (non-wetting) under zero gravity at a contact angle, the liquid (gas) will be trapped in the lower (upper) corner because of a lower gravitational potential energy when applying a downward gravity. Then, in this case, both the corner wetting (non-wetting) effect and the gravity effect tend to pull the liquid down to the bottom and, thus, competition between these two effects does not exist, leading to the non-occurrence of the re-entrant non-occlusion. The re-entrant non-occlusion does not exist for any contact angle in the case of $r_1 = 0.3$ in figure 8(*a*), because the identical upper and lower corners naturally have the equal corner effect (i.e. satisfy (2.17)), which identifies the same contact ranges for permitting the rounded corner wetting/non-wetting under zero gravity. Not limited to the case with the identical upper and lower corners, the conclusion of non-existence of the re-entrant non-occlusion is valid only if the upper and lower corners have the equal corner effect. Moreover, under the condition that the two corners have the equal corner effect and are at the same side (both the corners in the upper or the lower orientation), the competition between the corner wetting/non-wetting and gravity will exist, and the re-entrant non-occlusion is expected to exist, which is similar to the case of only one rounded corner.

For the cases shown in figure 8(*a*), changing r_1 from 0.3 to a smaller (not zero) or to a larger value makes the upper corner and the lower corner non-identical, which leads to the re-entrant non-occlusion for some contact angles. When $0 < r_1 < r_2 = 0.3$, the upper corner (with a smaller radius) has a stronger corner effect (i.e. has a larger contact angle

range for corner wetting/non-wetting under zero gravity) than the lower corner. For some contact angles, only the upper corner permits the corner wetting/non-wetting under zero gravity. Thus, in a downward gravity field, there exists a competition between the upper corner wetting effect and gravity effect to place the wetting liquid, which leads to the occurrence of the re-entrant non-occlusion for some wetting liquids (for $\gamma_l < \gamma < \gamma_{cr}$, where γ_l denotes the lower limit of the contact angle corresponding to two critical Bond numbers such as the contact angle value of point L on the black curve). By analogy, when $r_1 > r_2 = 0.3$, the lower corner (with a smaller radius) has a stronger corner effect. The competition between the lower corner non-wetting effect and gravity effect leads to the occurrence of the re-entrant non-occlusion for some non-wetting liquids (for $\gamma_{cr}^* < \gamma < \gamma_u$, where γ_u denotes the upper limit of the contact angle corresponding to two critical Bond numbers such as the contact angle value of point U on the blue curve).

To illuminate the effects of the orientations, the critical Bond number for different combinations of the orientation angles θ_1 and θ_2 are shown in figure 8(*b*). The two corners are set to have the non-equal corner effect, and corner 1 (with a smaller radius) has a stronger corner effect. From the result shown in figure 8(*b*), the re-entrant non-occlusion occurs for some wetting liquids when corner 1 is in an upper orientation (e.g. the case of $\theta_1 = 90°$), and it occurs for some non-wetting liquids when corner 1 is in a lower orientation (e.g. the cases of $\theta_1 = -45°$), while it disappears when $\theta_1 = 0°$. The orientation of the other corner θ_2 can only affect the contact angle range of the re-entrant non-occlusion to some degree (comparing the contact angle ranges between the green line, the blue line and the magenta line shown in the inset of figure 8*b*). The re-entrant non-occlusion mainly depends on θ_1 (for which the corner has a stronger corner effect), and the effect of θ_1 is similar to the effect of the corner orientation angle in the tube of only one corner (see figure 6).

According to the above results, we can conclude that for the tube with only two corners, the corner exhibiting a stronger corner effect plays the leading role in the re-entrant non-occlusion of the tube. The re-entrant non-occlusion occurs for some wetting (non-wetting) liquids when the stronger corner is in an upper (lower) orientation, whereas it will not appear in the tube when the stronger corner is in a landscape orientation. In the following, we keep $\theta_1 = 90°$ and $\theta_2 = -90°$.

3.2.2. *Two rounded corners with different corner angles*

Identifying the corner with a stronger corner effect (i.e. a larger contact angle range for corner wetting/non-wetting under zero gravity) is essential to analyse the phenomenon of re-entrant non-occlusion. As discussed in the previous section, when the two rounded corners have the same angle, that with a smaller radius has a stronger corner effect. Likewise, when the two rounded corners have the same radius, that with a smaller angle has a stronger corner effect. In the following, we discuss the two rounded corners that are not identical in both angle and radius.

Four representative cases of the critical Bond number for two non-identical rounded corners ($\alpha_1 = 30°$, $\alpha_2 = 90°$ and $r_1 \neq r_2$) are shown in figure 9(*a*). If both corners have too large radii (e.g. the case of $r_1 = 0.8$ and $r_2 = 0.8$ in figure 9*a*), corner wetting/non-wetting will not be permitted for any liquid under zero gravity in both corners and, thus, the re-entrant non-occlusion and the unconditional non-occlusion will not occur. Assuming that the corner wetting/non-wetting is permitted for a set of fixed geometric parameters ($\alpha_1 = 30°$, $\alpha_2 = 90°$ and $r_2 = 0.3$), by solving (2.17), we can determine a value of corner 1 as $r_{1,e}$ ($= 0.46$). Then, corner 1 with radius $r = r_{1,e}$ has an equal corner effect to

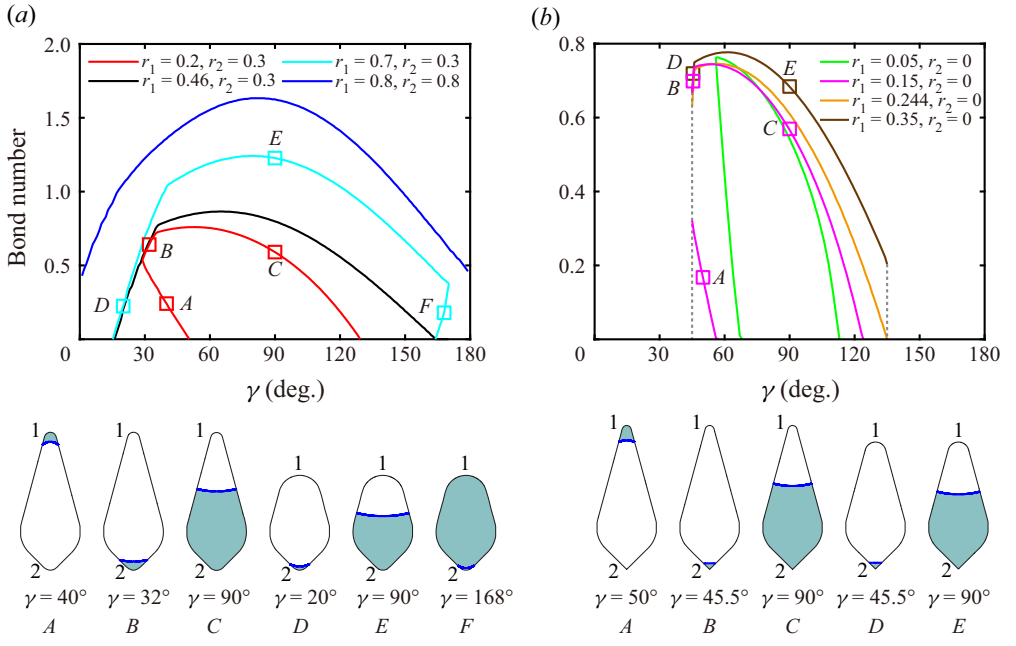

Figure 9. Critical Bond numbers of a horizontal tube with only two non-identical rounded corners ($\alpha_1 \neq \alpha_2$ and $r_1 \neq r_2$) with angles $\alpha_1 = 30°$ and $\alpha_2 = 90°$ at $\theta_1 = 90°$ and $\theta_2 = -90°$ for (*a*) different sets of rounding radii r_1 and r_2 and (*b*) $r_2 = 0$ and different values of r_1 versus contact angle. In (*b*), the grey dotted lines are the critical contact angles of the Concus & Finn (1969) condition with $\alpha_2 = 90°$, i.e. $\gamma = 45°$ and $\gamma = 135°$.

corner 2. Therefore, for the case of $r_1 = r_{1,e}$ (e.g. the case of $r_1 = 0.46$ and $r_2 = 0.3$ in figure 9*a*), the re-entrant non-occlusion does not occur for any contact angles. For $0 < r_1 < r_{1,e}$ (e.g. the case of $r_1 = 0.2$ and $r_2 = 0.3$ in figure 9*a*), corner 1 (i.e. the upper corner) has a stronger corner effect, and the re-entrant non-occlusion occurs for some wetting liquids. Likewise, for $r_1 > r_{1,e}$ (e.g. the case of $r_1 = 0.7$ and $r_2 = 0.3$ in figure 9*a*), corner 2 (i.e. the lower corner) has a stronger corner effect, and the re-entrant non-occlusion occurs for some non-wetting liquids. Note that the determination of the equivalent corner radius based on the zero Bond number is independent of the orientation angles θ_1 and θ_2 (obtained from (2.17)), which implies that the values of θ_1 and θ_2 have no effect on the comparison between the two corners.

For the tube with only one sharp corner, the re-entrant non-occlusion does not exist, and the unconditional non-occlusion occurs when satisfying the Concus & Finn (1969) condition (as the cases of $r = 0$ shown in figure 4*a–c*). However, for a tube with only two corners containing a sharp corner and a rounded corner, the re-entrant non-occlusion can exist when the rounded one has a stronger corner effect (e.g. the case of $r_1 = 0.05$ and $r_2 = 0$, and the case of $r_1 = 0.15$ and $r_2 = 0$ in figure 9*b*), whereas it cannot exist when the two corners have an equal corner effect (e.g. the case of $r_1 = 0.05$ and $r_2 = 0$, and the case of $r_1 = 0.15$ and $r_2 = 0$ in figure 9*b*) or the sharp one has a stronger corner effect (e.g. the case of $r_1 = 0.35$ and $r_2 = 0$ in figure 9*b*). In addition, when the contact angle satisfies the Concus & Finn (1969) condition for the sharp corner, the unconditional non-occlusion for the tube also occurs and the re-entrant non-occlusion does not exist. This is the reason why in the case of $r_1 = 0.15$ in figure 9(*b*), the re-entrant non-occlusion is limited in a contact angle range larger than $\gamma = 45°$.

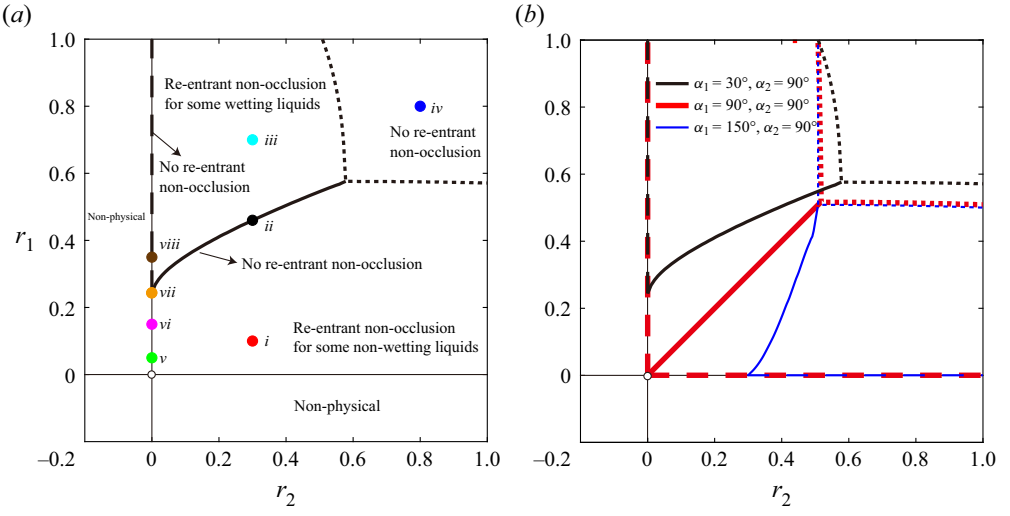

Figure 10. (*a*) Phase diagram of the re-entrant non-occlusion in a parameter space (r_1, r_2) for a horizontal tube with two non-identical rounded interior corners with angles $\alpha_1 = 30°$ and $\alpha_2 = 90°$ at $\theta_1 = 90°$ and $\theta_2 = -90°$ and (*b*) boundary lines in the parameter space (r_1, r_2) for different sets of angles of two corners $\alpha_1 = 30°$ and $\alpha_2 = 90°$, $\alpha_1 = 90°$ and $\alpha_2 = 90°$ and $\alpha_1 = 150°$ and $\alpha_2 = 90°$. In (*a*), the black dotted line is determined by (2.20), the black solid line is determined by (2.17), and the black dashed line starts from the intersection point between the black solid line and the vertical line $r_2 = 0$ and ends at (0, 1). Points *i*, *ii*, *iii* and *iv* are $(r_1, r_2) = (0.2, 0.3)$, (0.46, 0.3), (0.7, 0.3) and (0.8, 0.8), respectively, and correspond to the cases in figure 9(*a*). Points *v*, *vi*, *vii* and *viii* are $(r_1, r_2) = (0.05, 0)$, (0.15, 0), (0.244, 0) and (0.35, 0), respectively, and correspond to the cases in figure 9(*b*). The white circle denotes the origin $(r_1, r_2) = (0, 0)$. In (*b*), the meanings of the different line types are the same as those in (*a*), and the different line colours correspond to the cases for different (α_1, α_2).

3.2.3. *Phase diagram*

For a tube with two known corner angles α_1 and α_2, the existence of re-entrant non-occlusion in the radius parameter space (r_1, r_2) is shown in figure 10. Notably, we prescribe $\theta_1 = 90°$ and $\theta_2 = -90°$.

As shown in figure 10(*a*), the space is divided into different regions. The points on the black dotted line determined by (2.20) correspond to the limiting radii for the tube to permit corner wetting/non-wetting. Then, for the points in the region (in the upper right of the diagram) surrounded by the black dotted line, corner wetting/non-wetting cannot occur for any wettability under zero gravity and, thus, the re-entrant non-occlusion does not exist (for any contact angles). The points on the black solid line determined by (2.17) correspond to the two corners having an equal corner effect, for which re-entrant non-occlusion does not exist. The black solid line separates the region (with larger r_1) of re-entrant non-occlusion occurrence for some wetting liquids from the region (with smaller r_1) of re-entrant non-occlusion occurrence for some non-wetting liquids. The points on the black dashed line correspond to the tubes in which the sharp corner (corner 1) has a stronger corner effect and, thus, the re-entrant non-occlusion does not exist for these points. The origin denoted by the white circle corresponds to the special tube with two sharp corners, for which the re-entrant non-occlusion does not exist. In summary, except for the points in the no re-entrant non-occlusion region and the points on the boundary line.

The phase diagram shown in figure 10(*a*) can be regarded as the representative case for $\alpha_1 < \alpha_2$. In figure 10(*b*), the representative cases for $\alpha_1 > \alpha_2$ (i.e. the case of $\alpha_1 = 150°$

and $\alpha_2 = 90°$) and for $\alpha_1 = \alpha_2$ (i.e. the case of $\alpha_1 = 90°$ and $\alpha_2 = 90°$) are also given. Note that the re-entrant non-occlusion will never occur for the case of $\alpha_1 = \alpha_2$ (see the red curve in figure 10*b*) if one of the corners is sharp.

3.3. *Discussion on multiple rounded corners*

The cases of one corner and two corners are the general cases for the study of how corners influence the existence of a re-entrant non-occlusion. The conclusions of these cases can be generalised and applied to predicting cases of multiple corners (e.g. the cases of three corners and four corners) in an open tube. First, the rounded corner wetting/non-wetting permitted under zero gravity is necessary for the existence of the re-entrant non-occlusion for a lower Bond number. Second, the competition between the rounded corner wetting/non-wetting effect and gravity effect can lead to the re-entrant non-occlusion. Third, deduced from the results of two-corner cases, the corner with the strongest corner effect (i.e. having the largest contact angle range for corner wetting/non-wetting under zero gravity) will play the leading role in the re-entrant non-occlusion. Based on these points, a qualitative analysis of the re-entrant non-occlusion of a tube with multiple rounded corners can be conducted by following the steps below.

First, based on (2.18), determine whether the corner wetting/non-wetting in the tube at a zero Bond number is permitted, and if not, then the re-entrant non-occlusion will not exist.

If (2.18) is satisfied, we then obtain the critical contact angles of each corner by solving (2.16) and determining which corner(s) has the strongest corner effect. Note that if the corner(s) with the strongest corner effect satisfies $r = 0$ (sharp corner), then the re-entrant non-occlusion will not exist.

Finally, according to the orientation of the determined rounded corner(s) with the strongest corner effect, we analyse the competition between corner wetting/non-wetting and gravity to determine whether the re-entrant non-occlusion exists. Specifically, the re-entrant non-occlusion is expected to exist for some wetting liquids for the corner(s) with the strongest corner effect at the upper side in the orientation angle range (0, 180°), whereas it will exist for some non-wetting liquids for the corner(s) at the lower side in the orientation angle range (−180°, 0°).

4. Conclusions

The capillary state in a horizontal open tube with corners in a downward gravity field has been theoretically investigated. When the rounded corner in a tube satisfies the rounded corner wetting/non-wetting condition, an interesting phenomenon regarding the re-entrant non-occlusion can occur for the tube, i.e. the capillary plug exists only for some medium Bond numbers, whereas the capillary non-occlusion is determined for sufficient low or high Bond numbers. In contrast, for the sharp corner in a tube, once satisfying the Concus & Finn (1969) condition, the capillary plug cannot form regardless of the Bond numbers and, thus, the re-entrant non-occlusion does not occur. These results indicate a difference in the performances of a rounded corner and a sharp corner with respect to the capillary statics.

Tubes with only one corner and two corners are focused on, and the conditions under which a re-entrant non-occlusion possibly exists are obtained. Above all, when a re-entrant non-occlusion occurs, the rounded corner wetting/wetting under zero gravity must be permitted in the tube, which requires the radius of the rounded corner r to be not so large but also not zero (i.e. not a sharp corner). For a tube with only one

rounded corner permitting the corner wetting, the re-entrant non-occlusion depends on the corner orientation (i.e. the value of θ). For an upper orientation ($0° < \theta < 180°$), the re-entrant non-occlusion occurs for some wetting liquids (some contact angles γ below 90°), and for a lower orientation ($-180 < \theta < 0°$), the re-entrant non-occlusion occurs for some non-wetting liquids (some contact angles γ above 90°), whereas for a landscape orientation ($\theta = 0°$ or 180°), it cannot occur.

For a tube with only two corners, when the corners have an equal corner effect (i.e. have the same contact angle range for corner wetting/non-wetting under zero gravity), the re-entrant non-occlusion is expected to exist only for the special case of both corners at the same side (both the corners in the upper or the lower orientation). When the two corners have a non-equal corner effect, the re-entrant non-occlusion mainly depends on the corner with a stronger corner effect (i.e. having a larger contact angle range for corner wetting/non-wetting under zero gravity). If the stronger one is rounded (not sharp) and is not in a landscape orientation, a re-entrant non-occlusion will exist, which is similar to the case with only one corner.

Furthermore, according to the conclusions on the one-corner case and two-corner case, a qualitative discussion on the case of multiple (more than two) corners is provided. It is hoped that this paper lays a solid foundation for capillary non-occlusion and the vertical shift of droplets (so long as they are not spilled out) in optofluidic/microfluidic applications.

Supplementary material. Supplementary material are available at https://doi.org/10.1017/jfm.2023.1014.

Funding. This research was supported in part by the National Natural Science Foundation of China (no. 11972170).

Declaration of interests. The authors report no conflict of interest.

Author ORCIDs.
Dongwen Tan http://orcid.org/0000-0002-2205-3045;
Xinping Zhou http://orcid.org/0000-0001-6340-5273.

Appendix A. The Concus & Finn (1969) condition for a sharp corner in a transverse body force field

Consider the wetting liquids ($\gamma < 90°$). In a sharp corner of a tube in a transverse body force field (taking the downward gravity field as an example, see figure 11), a straight line Γ_p is specified as a special surface of liquid that is perpendicular to the axis of symmetry of the corner. The wetting perimeter and liquid area are denoted by Σ_p^* and Ω_p^*, respectively, which are given by

$$|\Sigma_p^*| = \frac{|\Gamma_p|}{\sin(\alpha/2)}, \quad |\Omega_p^*| = \frac{|\Gamma_p|^2}{4\tan(\alpha/2)}. \tag{A1a,b}$$

By substituting (A1a,b) into (2.4), the energy functional for the indicated liquid configuration can be given by

$$\Phi_p = |\Gamma_p|\left(1 - \frac{\cos\gamma}{\sin(\alpha/2)}\right) + |\Gamma_p|^2\left(\frac{l_{ca}^{-2}y_p^* + \lambda}{4\tan(\alpha/2)}\right), \tag{A2}$$

where y_p^* denotes the y coordinate of the liquid area Ω_p^*.

When $|\Gamma_p|$ is an infinitesimal (i.e. $|\Gamma_p| \to 0$), the second term on the right-hand side of (A2) is a higher-order infinitesimal, which could be omitted. Then, if the condition

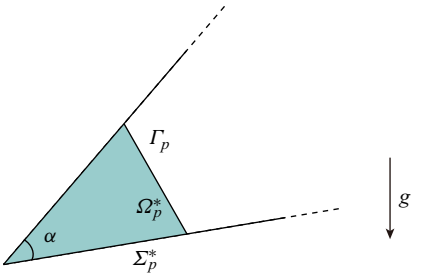

Figure 11. Schematic of a non-occluded liquid configuration in a corner of a tube in a transverse body force field.

$\gamma < (\pi - \alpha)/2$ is satisfied, one obtains

$$\Phi_{min} \leq \Phi_p < 0, \tag{A3}$$

which indicates the liquid non-occlusion of the tube. Regarding the non-wetting liquids ($\gamma > 90°$), based on a similar derivation, the liquid non-occlusion of the tube will also be determined when satisfying the condition $\gamma > (\pi + \alpha)/2$.

The corner orientation and the strength of gravity field do not affect the above derivation. Therefore, we can conclude that when a tube contains the sharp corner satisfying the Concus & Finn (1969) corner condition (i.e. $\gamma < (\pi - \alpha)/2$ or $\gamma > (\pi + \alpha)/2$), the liquid non-occlusion will occur in the tube regardless of the corner orientation and the strength of the gravity field.

Appendix B. Reduction of non-occluded liquid configurations under zero gravity

Under zero gravity, the interface determined by the 2-D Young–Laplace equation (2.6) and the contact angle condition (2.7) is a circular arc Γ with radius $R_s = 1/\lambda$. It is possible to theoretically exclude the circular arcs solutions that cannot minimise the energy functional (2.4). This appendix is based on the theorems and corollary from Finn (1986) to exclude the non-minimising configurations in the tube geometries described in § 2.1 under zero gravity.

Finn (1986) conducted formal mathematical research on the minimal interface problem under zero gravity conditions and obtained a series of theorems, corollaries and lemmas. Based on the theorems and corollary in Finn (1986), Concus & Finn (1990) excluded the non-minimising configurations in a rounded rectangle-shaped cross-section, and Fischer & Finn (1993) excluded the non-minimising configurations in a modified proboscis-shaped cross-section.

Here, dispensing with the corresponding mathematical derivation, we quote the theorems and corollary from Finn (1986). The theorems and corollary to be used are as follows. Theorem 6.11 in Finn (1986) states the following: if the contact angle satisfies $0° < \gamma < 90°$, then on any minimising arc Γ there holds $2\delta < 180°$, where δ is half of the circular arc angle of Γ (see figure 12*a*). Corollary to Theorem 6.12 in Finn (1986) states the following: if $\gamma > 0°$ and if the curvatures k_1 and k_2 at the intersections with the boundary Σ of every minor arc Γ satisfy $(k_1 + k_2)R_s \geq 2\cos\gamma$, then there exists a solution of the occluding surface. Theorem 6.16 (second half) in Finn (1986) is as follows: if $k_1 + k_2 \geq 0$ and if $\delta + \gamma > \pi/2$, then Γ cannot yield a minimum.

Based on the above theorems or corollary, a tube with only two rounded corners is taken as an example to discuss the energy-minimising configuration in the tube. We first

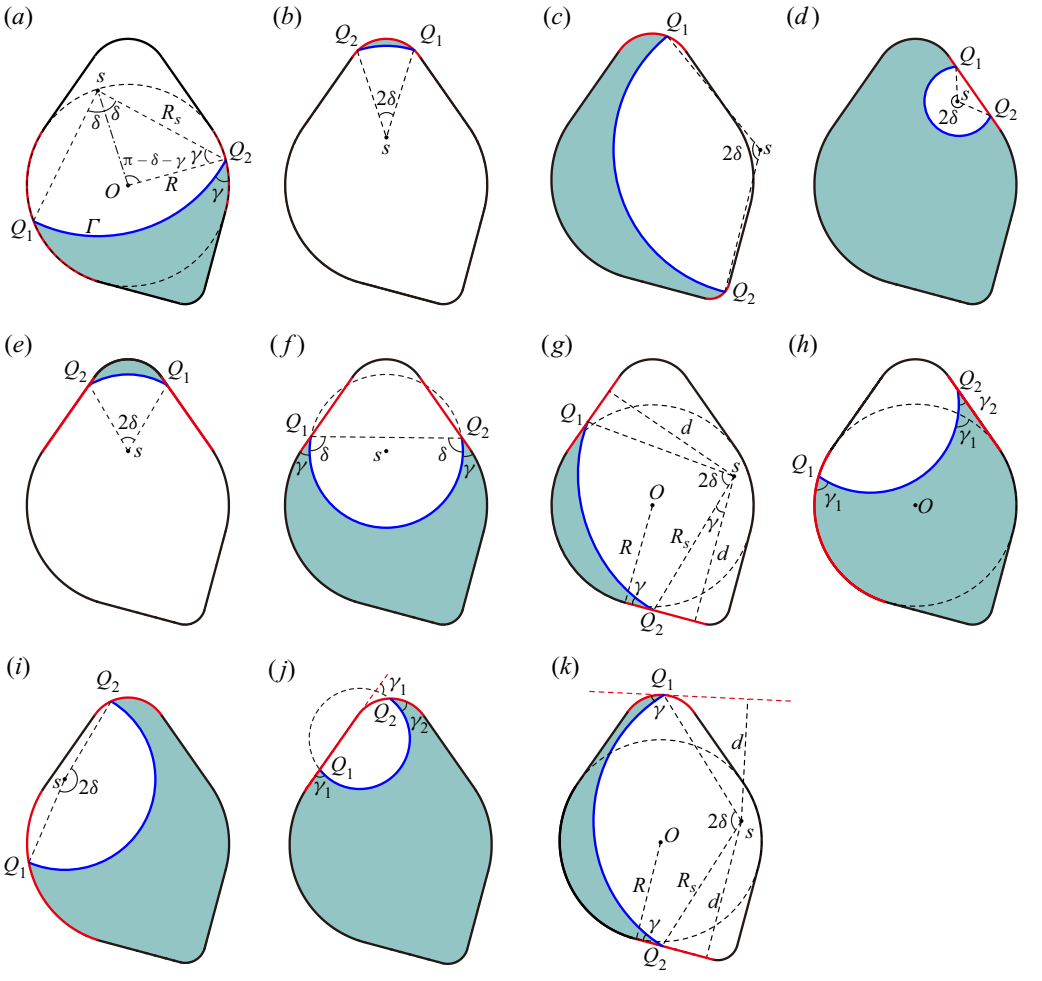

Figure 12. The non-occluded liquid configurations possibly exist in a tube with two rounded corners with contact angles of $0 < \gamma < \pi/2$. Representative cases of six types of configurations (the classification of the types depends on the locations of the contact points Q_1 and Q_2): case 1 for (*a*) in which both Q_1 and Q_2 are located on the arcs of the circle, case 2 for (*b*,*c*) in which both Q_1 and Q_2 are located on the arcs of rounded corners, case 3 for (*d*–*g*) in which both Q_1 and Q_2 are located on straight edges, case 4 for (*h*) in which Q_1 is located on arcs of the circle and Q_2 is located on a straight edge, case 5 for (*i*) in which Q_1 is located on the arcs of the circle and Q_2 is located on the arc of a rounded corner and case 6 for (*j*,*k*) in which Q_1 is located on a straight edge and Q_2 is located on the arc of a rounded corner. The red lines denote the parts on which the contact points are located. The dot-dashed line in (*a*) denotes the internal bisector of the circular arc angle of Γ. Here s and R_s are the centre and the radius of the interface Γ respectively, which becomes a circular arc in zero gravity, δ is half of the circular arc angle of Γ and d is the distance from s to the straight edge on which the contact point is located.

list all the typical non-occluded liquid configurations that may exist in the tube. The non-occluded liquid configurations are classified based on the location of the contact points. There are at most six combinations between the two contact points (Q_1 and Q_2) and the three different parts of a tube (i.e. the arcs of the circle, the arcs of the rounded corners and the straight edges of the corners), which correspond to the six types of cases for non-occluded liquid configurations. The discussion about excluding the non-minimising

configuration is conducted based on the six types of cases in which subcases may exist.

For simplicity, we only consider Γ to be a minor arc ($2\delta < \pi$), which is a necessary condition for a minimising configuration according to Theorem 6.11 in Finn (1986). We only discuss the wetting cases ($\gamma < 90°$), as the results of the wetting cases can be extended to the non-wetting cases ($\gamma < 90°$). The representative cases for the six types of non-occluded liquid configurations are shown in figure 12.

1. Γ meets Σ with both contact points at the arcs of the circle (figure 12*a*). For a minor arc Γ, this configuration can only occur if $R_s > R$, which contradicts Corollary to Theorem 6.12 in Finn (1986). Thus, this configuration can be excluded.
2. Γ meets Σ with both contact points on the arcs of the rounded corners.
   A. The two contact points are located on the arc of the same corner (figure 12*b*). For a minor arc Γ, this subcase can only occur if R_s is larger than the radius of the corner arc, which contradicts the Corollary to Theorem 6.12 in Finn (1986), similar to case 1. Thus, this subcase can be excluded.
   B. The two contact points are located on different corners (figure 12*c*). For a minor arc Γ (figure 12*c*), this subcase can only occur if R_s is larger than the radii of both rounded corners and thus can be excluded, similar to case 1.
3. Γ meets Σ with both contact points at the straight edges.
   A. The two contact points are located on the same edge (figure 12*d*). This subcase can occur only when $2\delta < \pi$ is satisfied, which contradicts Theorem 6.11 in Finn (1986). Thus, it can be excluded.
   B. The two contact points are located on different edges of a corner with liquid confined in the corner (figure 12*e*). This subcase cannot be excluded.
   C. The two contact points are located on different edges of a corner without liquid confined in the corner (figure 12*f*). For this subcase, we can easily obtain $\delta + \gamma > \pi/2$ for the configuration. Note that $k_1 = k_2 = 0$; then, this subcase can be excluded according to Theorem 6.16 in Finn (1986).
   As $k_1 + k_2 \geq 0$ is always satisfied for any liquid configuration in this tube and the comparison between $\delta + \gamma$ and $\pi/2$ can be easily given, the configurations with $\delta + \gamma > \pi/2$ are excluded and not discussed individually in the following cases for simplicity.
   D. The two contact points are located on different edges from different corners (figure 12*g*). For a minor arc Γ with $\delta + \gamma \leq \pi/2$, the only configuration may exist for this subcase, as shown in figure 12(*g*). Define $d = R_s \cos\gamma$ as the distance from s to an edge that Γ meets; then, the relation $d > R$ is necessary for the configuration. However, we can easily obtain the contrary that $R_s < R/\cos\gamma$ from the expression (2.12) of R_s and, thus, this subcase cannot actually occur and can be excluded.
4. Γ meets Σ with Q_1 at the arc of the circle and Q_2 at a straight edge (figure 12*h*). For this subcase, we can obtain $\gamma_1 \neq \gamma_2$ and, thus, it can be excluded.
5. Γ meets Σ with Q_1 at the arc of the circle and Q_2 at the arc of a corner (figure 12*i*). For a minor arc Γ, this case can only occur if R_s is larger than the radius of the circle and the radius of the corner and, thus, can be excluded, similar to case 1.
6. Γ meets Σ with Q_1 on a straight edge and Q_2 on the arc of a corner.
   A. The straight edge is tangent to the arc of the corner (figure 12 *j*). For this subcase, we can obtain $\gamma_1 \neq \gamma_2$ and, thus, it can be excluded.
   B. The straight edge is not tangent to the arc of the corner (figure 12*k*). For a minor arc Γ with $\delta + \gamma \leq \pi/2$, the only configuration may exist for this subcase, as

shown in figure 12(*k*). Similar to subcase 3D, the relation $d > R$ is necessary for this configuration but contrary to (2.12), and this subcase cannot actually occur and can be excluded.

In conclusion, only subcase 3B (i.e. the 'corner liquid configuration', in which the contact points are located on different straight edges of a corner and the liquid is confined in the corner) is reserved for the tube with contact angle $0 < \gamma < 90°$ under zero gravity. Note that the above discussion covers all types of liquid configurations and is not limited to tubes with two corners. This conclusion is applicable to the tube with n rounded corner(s) constructed as described in § 2.1.

References

Bhatnagar, R. & Finn, R. 2016 On the capillarity equation in two dimensions. *J. Math. Fluid Mech.* **18**, 731–738.

Brakke, K.A. 1992 The surface evolver. *Exp. Maths* **1**, 141–165.

Chen, Y. & Collicott, S.H. 2004 Investigation of the symmetric wetting of vane-wall gaps in propellant tanks. *AIAA J.* **42**, 305–314.

Chen, Y. & Collicott, S.H. 2006 Study of wetting in an asymmetrical vane-wall gap in propellant tanks. *AIAA J.* **44**, 859–867.

Concus, P. & Finn, R. 1969 On the behavior of a capillary surface in a wedge. *Proc. Natl Acad. Sci. USA* **63**, 292–299.

Concus, P. & Finn, R. 1987 Continuous and discontinuous disappearance of capillary surfaces. In *Variational Methods for Free Surface Interfaces* (ed. P. Concus & R. Finn), pp. 197–204. Springer.

Concus, P. & Finn, R. 1990 Dichotomous behavior of capillary surfaces in zero gravity. *Microgravity Sci. Technol.* **III** (2), 87–92.

Concus, P. & Finn, R. 1992 On accurate determination of contact angle. In *Microgravity Fluid Mechanics* (ed. H.J. Rath), pp. 19–28. International Union of Theoretical and Applied Mechanics. Springer.

Finn, R. 1986 *Equilibrium Capillary Surfaces*. Springer.

Fischer, B.S. & Finn, R. 1993 Existence theorems and measurement of the capillary contact angle. *Z. Anal. Anwend.* **12**, 405–423.

Manning, R., Collicott, S. & Finn, R. 2011 Occlusion criteria in tubes under transverse body forces. *J. Fluid Mech.* **682**, 397–414.

Manning, R.E. & Collicott, S.H. 2015 Existence of static capillary plugs in horizontal rectangular cylinders. *Microfluid Nanofluid* **19**, 1159–1168.

Mirski, M.A., Lele, A.V., Fitzsimmons, L. & Toung, T.J.K. 2007 Diagnosis and treatment of vascular air embolism. *Anesthesiology* **106**, 164–177.

Parry, A.O., Rascón, C., Jamie, E.A.G. & Aarts, D.G.A.L. 2012 Capillary emptying and short-range wetting. *Phys. Rev. Lett.* **108** (24), 246101.

Pour, N.B. & Thiessen, D.B. 2019 Equilibrium configurations of drops or bubbles in an eccentric annulus. *J. Fluid Mech.* **863**, 364–385.

Rascón, C., Parry, A.O. & Aarts, D.G.A.L. 2016 Geometry-induced capillary emptying. *Proc. Natl Acad. Sci. USA* **113**, 12633–12636.

Smedley, G. 1990 Containments for liquids at zero gravity. *Microgravity Sci. Technol.* **3**, 13–23.

Tan, D., Zhou, X., Zhang, G., Zhu, C. & Fu, C. 2022 Eccentricity effect on horizontal capillary emptying. *J. Fluid Mech.* **946**, A7.

Verma, G., Saraj, C.S., Yadav, G., Singh, S.C. & Guo, C. 2020 Generalized emptying criteria for finite-lengthed capillary. *Phys. Rev. Fluids* **5**, 112201(R).

Zhang, F.Y., Yang, X.G. & Wang, C.Y. 2006 Liquid water removal from a polymer electrolyte fuel cell. *J. Electrochem. Soc.* **153**, A225–A232.

Zhou, X., Zhang, G., Zhu, C., Tan, D. & Fu, C. 2021 Inside rod induced horizontal capillary emptying. *J. Fluid Mech.* **924**, A23.

Zhu, C., Zhou, X. & Zhang, G. 2020 Capillary plugs in horizontal rectangular tubes with non-uniform contact angles. *J. Fluid Mech.* **901**, R1.